Journal of the Royal Society of Western Australia, 74, 1991, 35-45

Eastern boundary currents of the southern hemisphere

A F Pearce

CSIRO Division of Oceanography, PO Box 20, North Beach, WA 6020, Australia

Abstract

Traditional atlases show ocean currents forming anti-clockwise gyres in each of the three southern hemisphere oceans, with northwards currents along the west coasts of the continents (the so-called Eastern Boundary Currents). Associated with the equatorwards currents and winds, cool upwelled water is found along the west coasts of southern Africa and South America. However, sea temperature charts reveal that there is in fact a southwards flow off Western Australia, and, despite net equatorwards winds which favour upwelling, there is no large-scale upwelling off this coast.

In this paper, the oceanic circulation in each of the Humboldt (Peru/Chile), Benguela (southern Africa) and Leeuwin (Western Australia) current systems is reviewed. Seasonal sea temperature patterns at the same latitudes clearly show the different thermal regimes operating, with important consequences for the marine biota.

The main features of the Leeuwin Current system are summarised, with emphasis on the mesoscale (10's to 100's km) meander/eddy structure as revealed by satellite imagery. Inter-annual variability in sealevel, which is an indicator of the strength of the Leeuwin Current, is linked with El Niño/ Southern Oscillation (ENSO) phenomena.

Introduction

The West Wind Drift current, driven eastwards around the globe by the strong westerly winds in the Southern Ocean, links the south Indian, Pacific and Atlantic Oceans. In the tropics, the westward-flowing South Equatorial Currents are driven by southeast trade winds. In consequence, there is an anti-clockwise gyre in each of the three southern hemisphere oceans, with relatively intense southwards (or polewards) currents along their western boundaries and weaker equatorwards flows in the eastern boundary current (EBC) regions (Wooster & Reid 1963).

Such is the picture painted by traditional current atlases (see, for example, Tchernia 1980). In the eastern South Atlantic Ocean, there is the equatorwards flow in the Benguela system, while the Humboldt Current system transports cool temperate water northwards off Chile and Peru. Associated with each of these two major current systems is seasonal upwelling of cooler, nutrient-rich subsurface water onto the continental shelf, leading to highly productive waters and rich fisheries.

By contrast, oceanographers have known for decades that the situation off Western Australia is different (Cresswell 1991), with warm water of tropical origin flowing southwards and a distinctive lack of large-scale and persistent upwelling.

This paper briefly reviews the broad-scale circulation off the western coasts of southern Africa and South America, and then focuses on the differences between these two "typical" eastern boundary currents and the anomalous Leeuwin Current. For further information on EBCs in general, the reader is referred to Wooster & Reid (1963) and Neshyba *et al.* (1989).

Large-scale oceanography

The difference between the three southern hemisphere EBCs is effectively illustrated by the mean sea surface temperature (SST) charts for summer and winter (Figs. 1 and 2 respectively).

The northwards deflection of the surface isotherms off Chile and Namibia indicate both the equatorwards flow of cool water from the south and the upwelling of cold subsurface water. Upwelling in both areas is most intense during the summer months, shown by the closed isotherms along the Peru coast between the equator and 15°S, and between 20 and 35°S off southern Africa (Fig. 1). In winter, the westwards extension of the isotherms along the equator reflects the flow in the South Equatorial Current systems (Fig. 2).

Off Western Australia, by contrast, there is a poleward deflection of the isotherms in both seasons (Figs. 1, 2) indicating the southwards advection of warm water, and there is no evidence of upwelling.

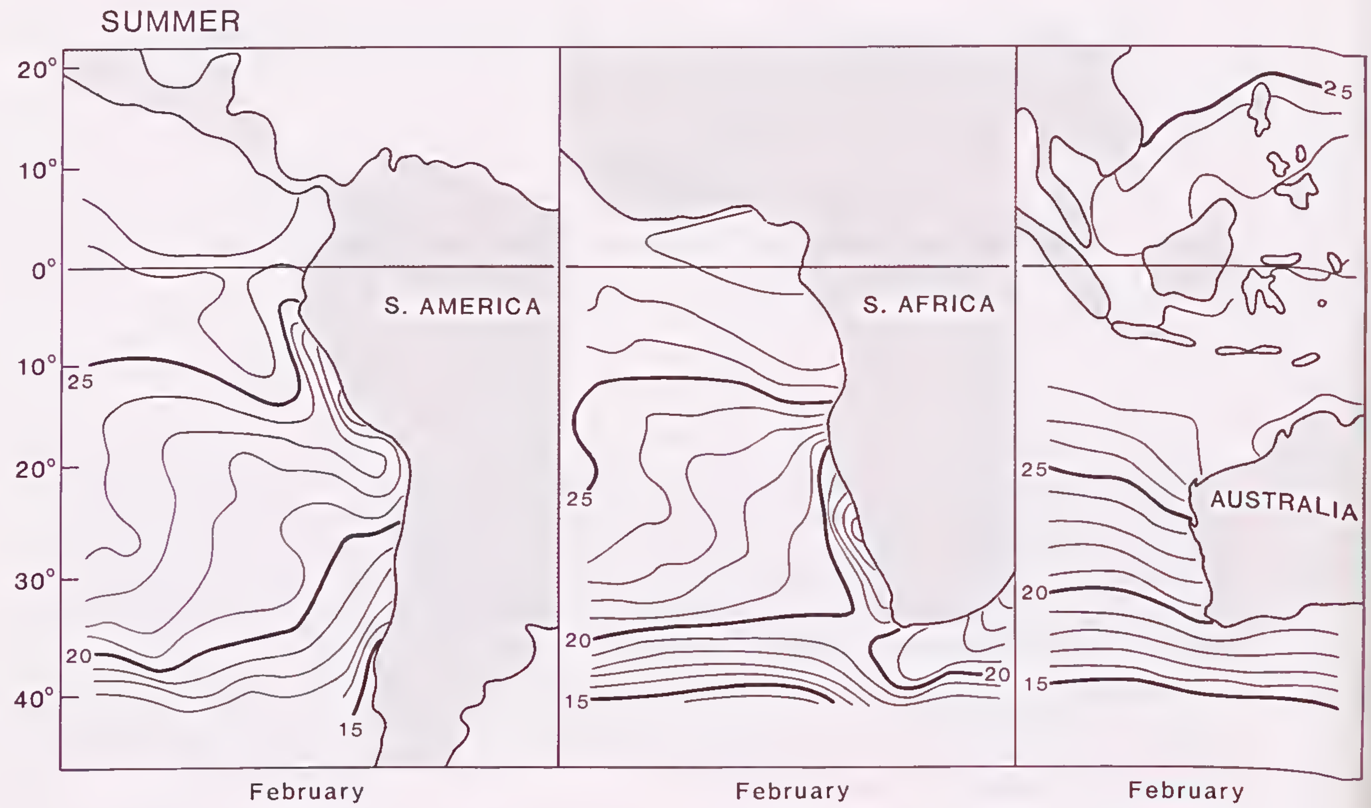

Figure 1 Summer (February) sea-surface temperature charts off the western coasts of South America, southern Africa and Australia (after Reynolds 1982).

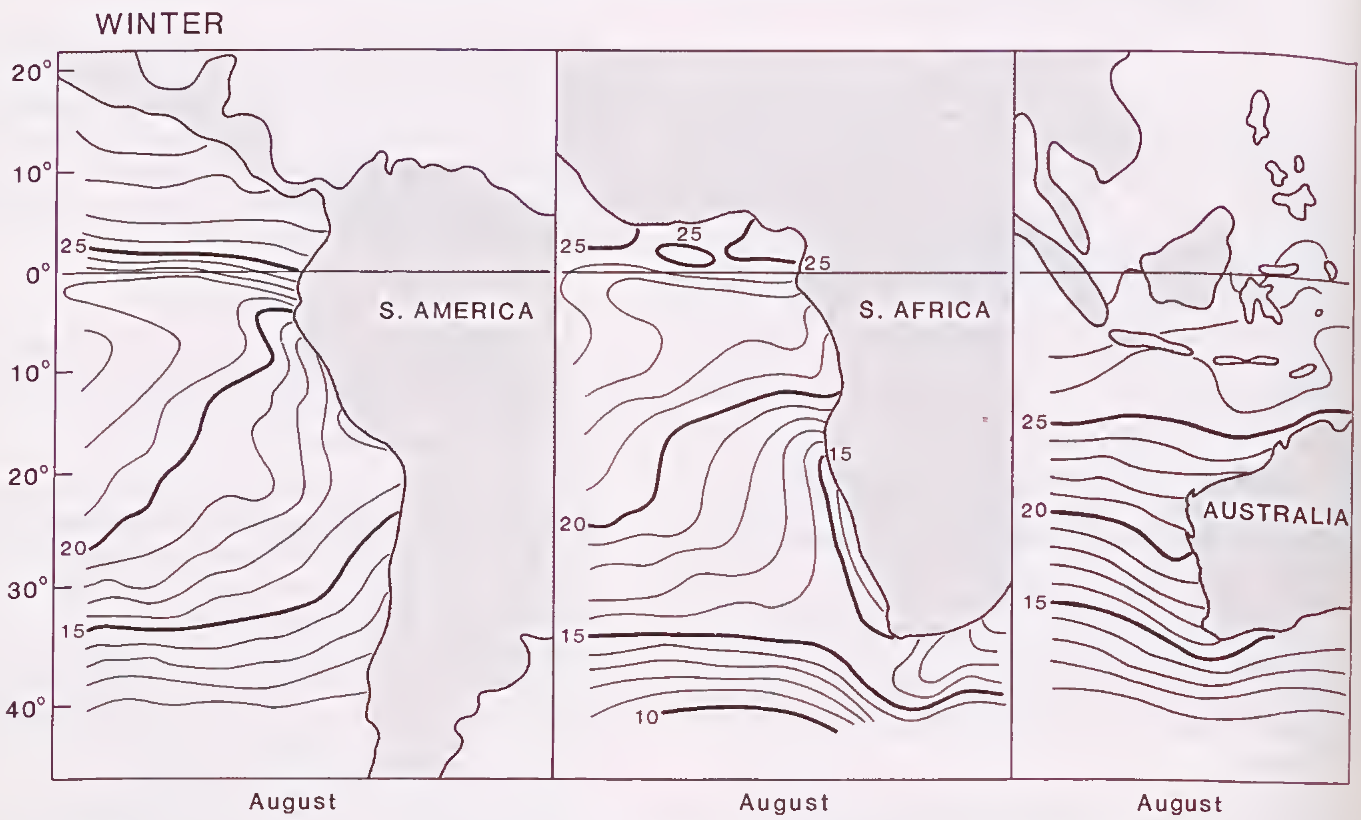

Figure 2 Winter (August) sea-surface temperature charts off the western coasts of South America, southern Africa and Australia (after Reynolds 1982).

Gentilli (1972) illustrated the different thermal regimes in the three areas using SST data derived from ocean atlases. More recent information using the Combined Ocean/Atmosphere Data Set (COADS) enables the zonal surface temperature to be examined on a monthly basis, and again the appreciable differences between the three EBC regions is apparent (Fig. 3; Table 1). In the three areas, the SST at 10 degrees of longitude (about 1000 km) offshore is not appreciably different: about 21°C in summer and 16°C in winter. Off Africa and South America, SST falls by about 3°C towards the coast as a result of the cool northwards flow and the upwelling. On approaching the Australian coast, however, SST rises by 1.5°C in February, and 3.2°C in August (when the Leeuwin Current is flowing strongly). Indeed, the waters near Western Australia are warmer in winter than those near Namibia and Chile in summer.

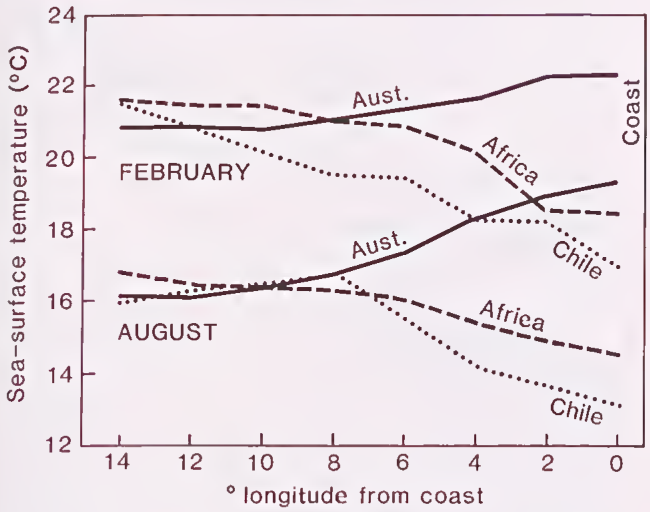

Figure 3 Gross surface thermal structure at 31°S off Western Australia, southern Africa and Chile, derived from COADS monthly data in 2 degree squares.

Table 1

Comparison of summer (February) and winter (August) SST's (°C) at latitude 31°S for the three EBC areas, derived from COADS.

EBC region	February	August
Benguela	18.4	14.5
Humboldt	17.0	13.0
Leeuwin	22.3	19.2

The subsurface structure is also grossly different. Godfrey & Ridgway (1985) have shown that the isotherms off Western Australia deflect downwards towards the continental slope, indicative of the southwards current, whereas off the other two southern hemisphere west coasts there is a strong upward deflection associated both with the northward current and the upwelling.

Primary production (Fig. 4, from FAO 1981) is strong both off Namibia, where production averages over 500 mg carbon $m^{-2} d^{-1}$ in the upwelling region, and off Peru, reaching 500 mg carbon $m^{-2} d^{-1}$ in an isolated patch but generally in the range 250 to 500 mg carbon $m^{-2} d^{-1}$. In west Australian waters, primary productivity is generally less than half the above values.

The abundance of zooplankton mirrors the geographical distribution of phytoplankton (Fig. 5). The Leeuwin Current is again seen to have a much lower biomass than the other two areas, but it is worth noting that there is still some coastal enrichment despite downwelling.

The Benguela system

The ocean circulation off the west coast of southern Africa has been described in some detail by Shannon (1985), who proposed a conceptual model of the Benguela system – Fig. 6 is a simplified version of the main features of the circulation. There is a broad (order 200 km wide, Nelson & Hutchings 1983) northwards drift of cool surface waters beyond the shelf with speeds of 10 to 30 cm s^{-1} (the classical Benguela Current), forming the eastern branch of the South Atlantic anticyclonic gyre. The volume flow in the Benguela Current is estimated to be between 10 and 16 Sv (1 Sv = $10^6 m^3 s^{-1}$; Shannon 1985).

A shelf-edge jet, first investigated by Bang & Andrews (1974), has been found to extend from south of Cape Town to a point near 31°S where it turns westward. This is a permanent baroclinic jet which has a width of some 10 km, extends down to 120 m and attains core velocities of 60 cm s^{-1} where the shelf is steepest.

Satellite-tracked buoys released off Cape Town during summer moved northwestwards and suggested that topographical steering plays an important role in the trajectory of the Current (Nelson & Hutchings 1983). Current speeds deduced from the buoy tracks were up to 35 cm s^{-1} in the shelf-edge jets. A branch of the Benguela Current continues to penetrate northwards along the coast as far as about 12°S, but the main body of water diverges from the coast and joins a warm saline flow from the north (the Angola Current) in moving westwards between latitudes 15 and 20°S. There is a frontal (convergence) zone between the cool waters of the Benguela system and the tropical/equatorial water of the Angola Current. The front varies seasonally in position and strength but generally lies between about 15 and 17°S and has a surface thermal gradient of about 4°C per 1° latitude (Shannon *et al.* 1987).

Further offshore between 0 and 5°E longitude, there appears to be a northwards meandering jet over the Walvis Ridge.

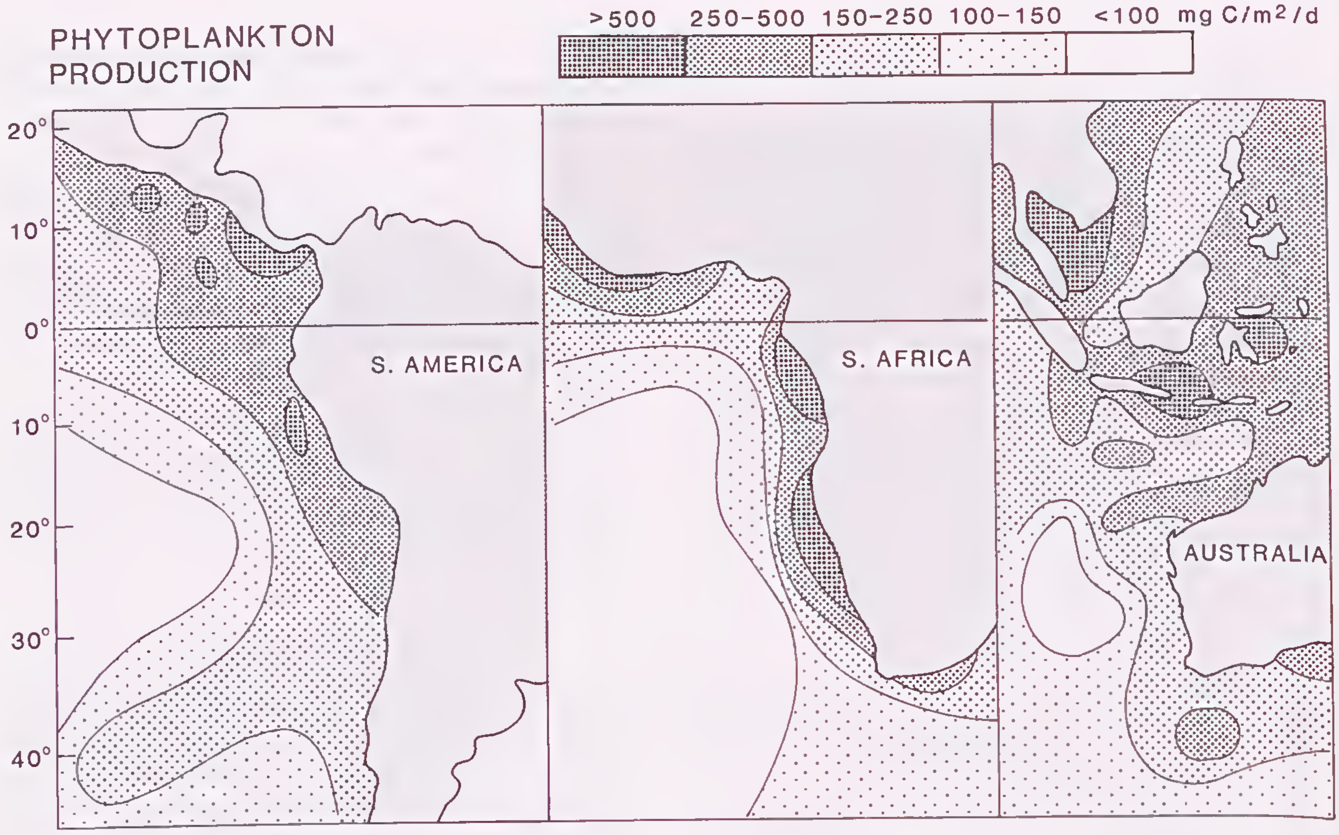

Figure 4 Phytoplankton production (mg C m^{-2} d^{-1}) off the western coasts of South America, southern Africa and Australia (after FAO 1981).

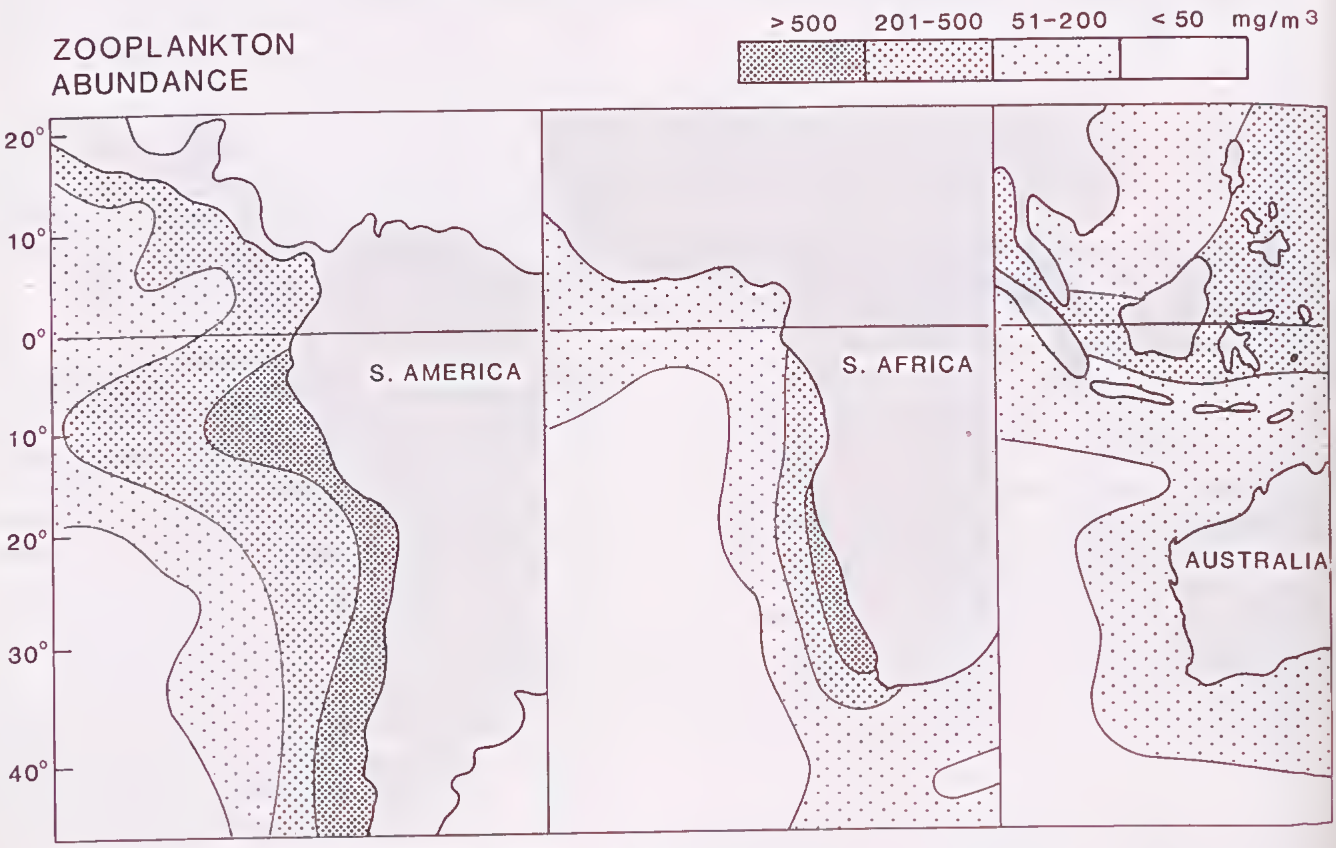

Figure 5 Zooplankton abundance (mg m^{-3}) off the western coasts of South America, southern Africa and Australia (after FAO 1981).

Below the surface there is a deeper poleward "compensation" countercurrent which reaches as far south as Luderitz at 27°S (Hart & Currie 1960); it is generally characterised by low oxygen content. Nelson (1989) has shown that there is in fact an ambient poleward undercurrent of some 5 cm s^{-1} flowing along the whole shelf, shelf-edge and slope regions. This current is modulated by barotropic coastal-trapped waves with two to five day periodicity. On the inner shelf, the flow attains speeds of 40 cm s^{-1} over short periods during the poleward phase. The destiny of the shallower poleward flow in the Cape Peninsula area, where the shelf is very narrow and the coastline turns westward, is unknown, but at least a part is known to follow the coast onto the Agulhas Bank. A part may retroflect into the shelf-edge jet.

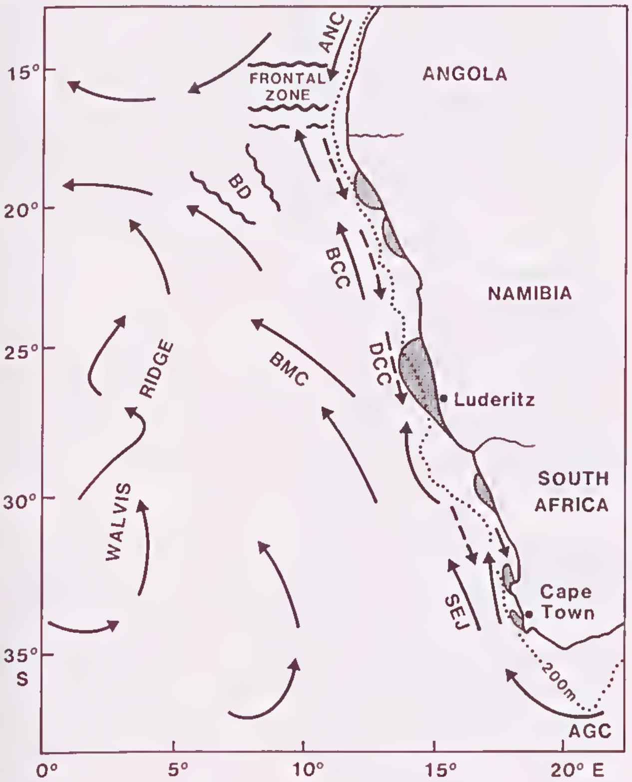

Figure 6 Conceptual model of the Benguela system, simplified from Shannon (1985). AGC = Agulhas Current, ANC = Angola Current, BCC = Benguela Coastal Current, BD = Benguela Divergence, BMC = Benguela Main Current, DCC = Deep Compensation Current, SEJ = Shelf-edge jet. Regions of locally enhanced upwelling are shaded. Solid arrows are surface currents, dashed are subsurface. The dotted line shows the 200 m contour.

The prevailing winds are from the south, and hence upwelling-favourable, although both seasonal and alongshore variations in wind stress occur. There are in fact two distinct regimes in the upwelling system, separated at about 31°S: the southerly region experiences a clear seasonal wind-driven upwelling pattern (upwelling is strongest in spring and summer when the northwards wind stress is strongest), whereas north of 31°S the upwelling is more perennial. The upwelling regime consists of a series of localised upwelling cells along the 1700 km of coastline between 20 and 35°S (the shaded near-coastal features in Fig. 6).

The Humboldt system

The Humboldt (or Peru-Chile) current system off South America is a classical eastern boundary upwelling region, exhibiting the characteristics of equatorward surface flows associated with wind-driven coastal upwelling, high biological productivity and rich fisheries. The upwelling is most pronounced off the Peru coast (4 to 18°S), which has, as a result, been studied in more detail than the Chilean region, and less information is available for the current regime south of 25°S. This review of the circulation in the upper few hundred metres is taken largely from Gunther (1936), Wyrtki (1963, 1966), Zuta (1988) and Codispoti *et al.* (1989). Authors differ in their conclusions on some aspects (partly a result of the different seasons in which surveys have been undertaken), but this synthesis attempts to summarise the main features of the circulation.

Surface currents off this coast are generally towards the north (Fig. 7) as described earlier. The Peru Oceanic Current (POC), which forms the eastern limb of the anti-cyclonic circulation of the South Pacific Ocean, extends to about 700 m depth. North of about 20°S, it diverges from the coast, flowing westwards south of 10°S and entraining or merging with water from the Peru Countercurrent (PCCC) and the Equatorial Countercurrent (SECC) as it returns westwards to form the South Equatorial Current (SEC). Wyrtki (1963) places the eastern limit of the POC off central Peru at about longitude 82°W. It consists largely of Subtropical Surface Water from the South Pacific Ocean, transporting about 8 Sv at 24°S increasing to 14 Sv as it heads westward (Wyrtki 1966).

Nearer the coast lies the northwards Peru Coastal Current (PCC), which is shallower (<200 m) than the POC. Its southern and northern limits vary seasonally, but lie approximately between about 33 & 40°S and 5 & 10°S respectively (Gunther 1936; Wyrtki 1963). Wyrtki (1963) considers that it lies east of about 78°W off central Peru; it transports about 6 Sv.

Between the two north-flowing currents, the Peru Countercurrent (PCCC) carries warm equatorial subsurface waters southward, commencing at the coast at about 5°S and then flowing almost due south along 80°W. It draws some of its water from the northern extremity of the Peru Coastal Current. It is about 250 km wide and extends down to about 500 m, but its maximum strength is at about 100 m depth. It is not always evident at the surface because of wind-driven surface currents. The PCCC transports about 11 Sv

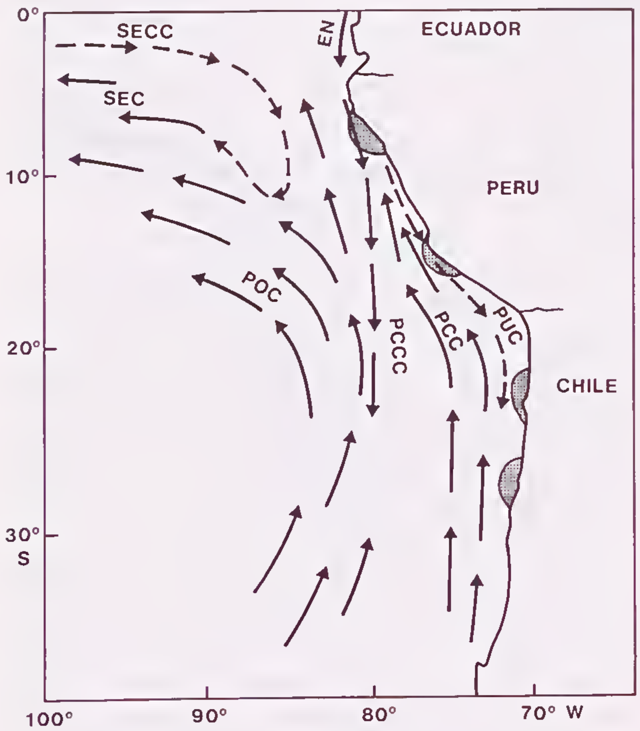

Figure 7 Simplified diagram of the main features of the ocean circulation off western south America, largely after Wyrtki (1966) and Zuta (1988). EN = El Niño Current, PCC = Peru Coastal Current, PCCC = Peru Countercurrent, POC = Peru Oceanic Current, PUC = Peru Undercurrent, SEC = South Equatorial Current, SECC = South Equatorial Countercurrent. Regions of supposedly enhanced upwelling (Gunther 1936) are shaded to illustrate the alongshore variability of upwelling. Solid arrows are surface currents, dashed are subsurface.

southwards at 6°S, and weakens to 6 Sv at 15°S and 2 Sv by the time it reaches 22°S.

Below the surface near the coast, there is the southward-flowing Peru Undercurrent (PUC), which is separate from the Peru Countercurrent further offshore (Wyrtki 1963, Brockman *et al.* 1980, Huyer *et al.* 1991). Poleward undercurrents of this nature, flowing counter to the dominant wind, are persistent and important features of most upwelling regions (Smith 1983). At 15°S, the Peru Undercurrent extends across the shelf under a thin (30 m) equatorward wind-driven surface layer, and down the upper slope to a depth of about 250 m and offshore extent less than 50 km from the shelfbreak. Maximum flow occurs between 50 and 150 m depth; the transport is about 1 Sv at 10°S (Huyer *et al.* 1991). The southern limit of the PUC has been estimated by Silva & Neshyba (1979) to lie at about 48°S.

Brattström & Johanssen (1983) have suggested that there is a Chile Coastal Countercurrent (which flows southwards) and a north-flowing Chile Coastal Current, both inshore of the Peru Undercurrent. These currents, which are present along sections of the Chilean coastline, have not been included in Fig. 7 for clarity.

The South Equatorial Countercurrent (SECC) carries some 11 Sv of low-salinity, warm equatorial surface water into the area from the west, as a surface/subsurface flow between about 4°S and 7°S. It deflects southwards at about 85°W, and then at about 15°S returns westwards and merges with the Peru Oceanic Current (Wyrtki 1963). Wyrtki (1966) has no mention of a countercurrent south of the equator, but shows an eastwards Undercurrent carrying 35 Sv along the equator; some of this returns westwards with the SEC, while the rest runs southward along the shelf as an undercurrent.

There is an intermittent poleward intrusion of warm, low salinity equatorial water down the coast of northern Peru (Murphy 1936), associated with interannual variations in the central and western Pacific. This nutrient-poor water generally manifests itself at about Christmas time, and has the traditional name of "El Niño" (or "the Christ-child"). At intervals of between 2 and 10 years, this intrusion is extensive and devastating, raising the temperature of the water by many degrees, lowering the thermocline and thus adversely affecting the upwelling process. Plankton and fish die and decompose, birds starve or leave the area, and the commercial fishery collapses. Such events are now known as "ENSO events", as the El Niño is in fact merely one manifestation of a chain of global oceanic and atmospheric phenomena associated with the Southern Oscillation, which is a major reversal of the atmospheric pressure fields in the Indian and Pacific Oceans (Quinn *et al.* 1978, Cane 1983).

In some localised regions, upwelling of nutrient-rich waters onto the continental shelf is stronger in autumn and winter (May to September) than in spring/summer (Zuta 1988). Instead of upwelling occurring simultaneously all along the coast, upwelling cells tend to develop with offshore scales of order 10's of kilometres (Smith 1983). Gunther (1936) describes the existence of locally enhanced upwelling cells which appear to be associated with highly variable anticyclonic eddy-like circulations along the coast, as a result of alongshore variations in both topography and wind stress. His observations agreed substantially with those of some earlier investigators, finding stronger upwelling centred at about 28°S, 23°S, 15°S and 7°S (Fig. 7). As pointed out by Wyrtki (1966), however, localised upwelling centres may in fact occur anywhere along the coast. The upwelling zones north of about 12°S are supplied by high salinity, low oxygen water in the poleward countercurrent PUC at depths of order 100 to 150 m; further south, the source of upwelled water is the lower layer of the less saline Peru Coastal Current (Wyrtki 1966). Both of these water masses are drawn up onto the shelf during upwelling events.

The difference in the general location of the strongest upwelling centres between Peru and Namibia reflects a similar variation in the strength of the offshore Ekman transport.

The Leeuwin system

In contrast with the above two classic EBCs, the Leeuwin Current exhibits many unusual features (Figs. 8,9).

The general anticyclonic flow which must complete the circuit of the southern Indian Ocean to maintain continuity of flow, takes about 3 years to complete the cycle; surface drift cards suggest that the mean current speed is about 17 cm s^{-1} (Shannon *et al.* 1973). In the southeastern region of the Indian Ocean, however, there is a large alongshore pressure gradient between the warm (low-density) equatorial waters and the cool (high-density) Southern Ocean (Thompson 1984 and Godfrey & Ridgway 1985). This meridional gradient, which is much stronger than that in the other corresponding eastern boundary current regions (Fig. 10), induces a net eastwards geostrophic flow from the Indian Ocean towards Australia, and the flow is then deflected down the pressure gradient by the continent to form the Leeuwin Current (Fig. 8).

Godfrey & Weaver (1991) suggest one reason that such a large gradient is found off Western Australia and not off any other eastern ocean boundary has to do with the existence of the open Indonesian passages. These result in vertical temperature profiles off the Northwest Shelf being very similar to those in the (very warm) western equatorial Pacific. The warm water supply leads to a loss of heat to the atmosphere and convective overturn of the water column between about 20 and 36°S, and hence to the unique alongshore pressure gradient of Fig. 10.

A summer feature, named the "West Australian Current" by Andrews (1977), meanders eastwards between latitudes of about 29 and 31°S, and deflects southwards offshore of the Leeuwin Current along the continental margin. This current appears to be a branch of the traditional northwards current of the same name which forms the eastern limb of the south Indian Ocean gyre, and it may perhaps be better to retain the name in its original usage. Andrews' current could be termed the "West Australian Summer Current" (Fig. 9).

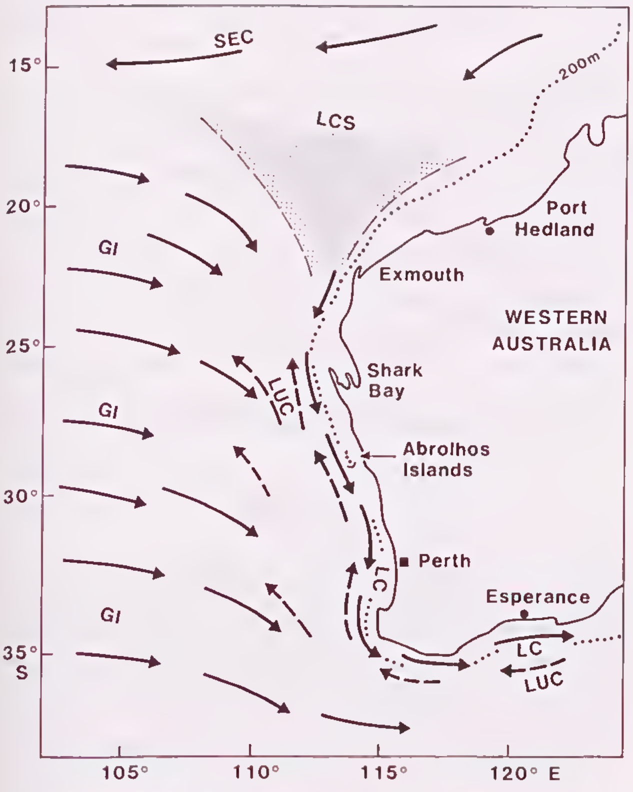

Figure 8 Schematic diagram of the main features of the Leeuwin Current system. GI = geostrophic inflow from the open ocean, LC = Leeuwin Current, LCS = Leeuwin Current source area, LUC = Leeuwin Undercurrent, SEC = South Equatorial Current. Solid arrows are surface currents, dashed are subsurface. The dotted line shows the 200 m contour.

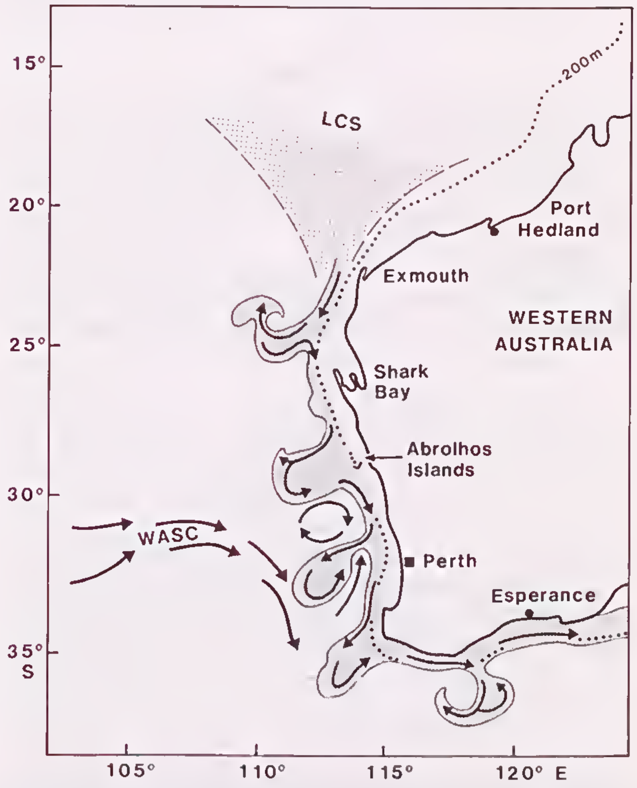

Figure 9 Schematic diagram of mesoscale features of the Leeuwin Current system, derived largely from satellite imagery. The Leeuwin Current itself is shaded, the solid arrows indicating the flow in the warm surface meanders and jets as well as the currents in the cooler offshore waters. WASC = West Australian Summer Current (modified from Andrews 1977). The dotted line shows the 200 m contour.

Despite equatorward (upwelling-favourable) winds (Godfrey & Ridgway 1984), there is no upwelling off Western Australia. This lack of upwelling is clearly illustrated by comparing the vertical structure of the upper water column on the continental shelf at about 32°S with that in the Benguela area (Fig. 11). In the Benguela, surface temperatures just beyond the shelf-break exhibit the expected seasonal pattern, with summer values of about 19°C falling to 15°C in winter. Closer inshore, however, in water depths of 80 to 150 m, the surface temperature is about 14°C in all months with minimal seasonal variation. Just 20 m below the surface, the temperature is about the same as at the surface during winter, but in summer it falls by almost 4°C as a result of the upwelling. There is, therefore, a reversed seasonal pattern below the surface off southern Africa, the water being warmer in winter than in summer (Fig. 11). Off Western Australia, by contrast, temperature measurements in 55 m water depth show that the column is well-mixed in all seasons, with mean summer temperatures of about 22°C falling to 19°C in winter.

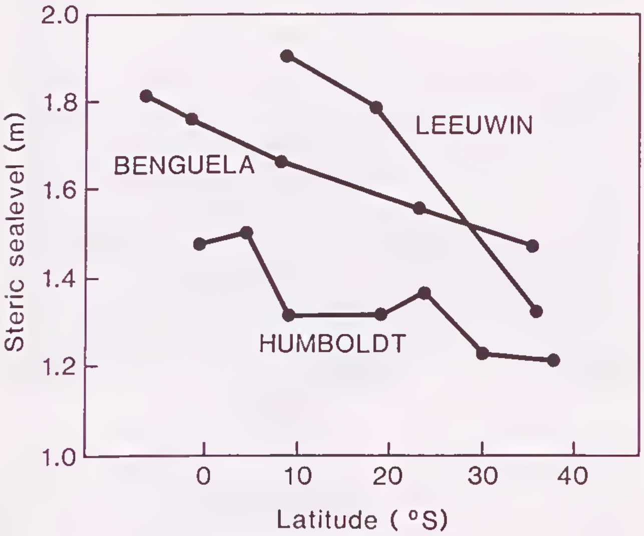

Figure 10 Alongshore sealevel difference on the eastern boundaries of the south Pacific, Indian and Atlantic Oceans (adapted from Godfrey & Ridgway 1985).

Thompson (1984) reported the existence of an equatorward undercurrent a few hundred metres below the Leeuwin Current off Shark Bay. This countercurrent, which transports high-salinity South Indian Central Water northward and offshore (Fig. 8), is also reflected in the geopotential topography of the 300 m surface relative to 1000 m (Wyrtki 1971).

LUCIE

The most comprehensive survey of the Leeuwin Current system to date was undertaken in 1986 and 1987, known as the Leeuwin Current Interdisciplinary Experiment (LUCIE). The following brief review draws from LUCIE papers by Church *et al.* (1989), Weaver & Middleton (1989) and Smith *et al.* (1991), as well as the important papers by Thompson (1984), Godfrey & Ridgway (1985) and Batteen & Rutherford (1990). It will concentrate on features of the Current south of Exmouth (22°S); the "source area" to the north has been dealt with by Church *et al.* (1989) and by Cresswell (1991). It should be pointed out that 1986/87 was an ENSO period, so the Leeuwin Current may not have been "typical" at that time (Pearce & Phillips 1988, Smith *et al.* 1991).

The Leeuwin Current is relatively narrow (200 km in the north, narrowing to 50 to 100 km in the south), and shallow (50 m in the north to 200 m in the south) (Church *et al.* 1989). It flows more strongly during the autumn, winter and early spring months than in summer. Peak current speeds can exceed 1.5 m s^{-1} (or 3 knots).

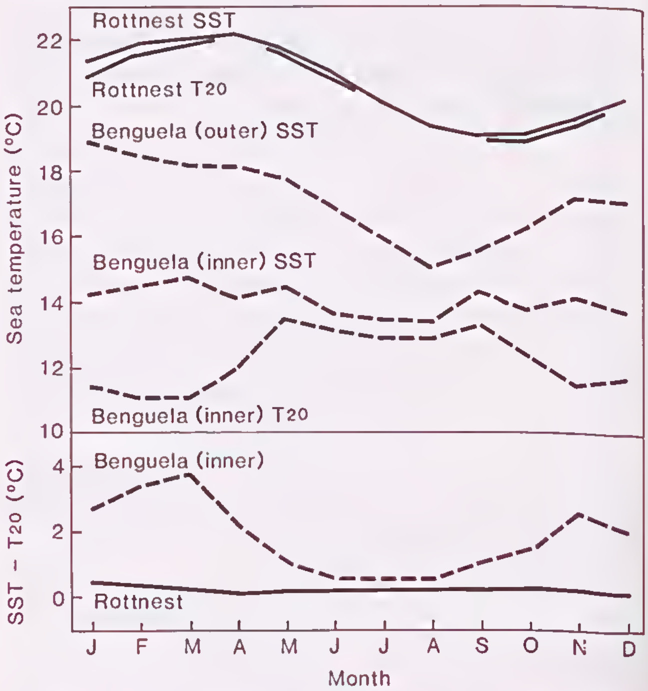

Figure 11 Comparison of the monthly mean thermal structure on the continental shelf at 32°S: Benguela and Leeuwin systems. The Benguela (inner) site was in 100 m water and the outer in 360 m depth (data from Buys 1957). The Leeuwin Current data is from 55m water depth. SST represents sea-surface temperature, T20 is the temperature at 20 m depth. The lower diagram depicts the thermal differential between the water surface and 20 m depth.

LUCIE results indicated that, near the Abrolhos Islands during the spring months, there was a net southward flow of 20 cm s^{-1} in the current core over the upper slope and a northwards undercurrent of 10 cm s^{-1} below about 300 m. In autumn, the southwards jet had strengthened to 55 cm s^{-1}, and the undercurrent was very much weaker than in spring. By winter, the alongshore flow to the south had moved further offshore but hydrographic measurements showed that it was still flowing very strongly. The flow in the upper 100 m of water just offshore of the shelfbreak near the Islands was remarkably persistent to the south between February and August. The southwards transport in the Current increased from 1.4 Sv in summer to almost 7 Sv in mid-winter.

Along the south coast, the Leeuwin Current was located just beyond the shelf-break (Cresswell & Peterson , unpubl.). A warm offshoot some 50 km wide and 130 m thick was transporting the warm water 200 km southwards into the Southern Ocean, the maximum speed being about 1 m s^{-1}. There was a westward undercurrent at a depth of 400 to 700 m, with a core speed of about 20 cm s^{-1}.

Satellite imagery

The pioneering satellite work of Legeckis & Cresswell (1981) directly confirmed earlier concepts of the southward transport of warm water and the seasonal nature of the Leeuwin Current. NOAA AVHRR (Advanced Very High Resolution Radiometer) satellite images received in Perth have subsequently shown the complex nature of the Leeuwin Current.

Superimposed on the narrow southwards flow of warm, low-salinity tropical water along the shelf-break is a series of wave-like meanders which transport Leeuwin Current water away from and back towards the coast (Fig. 9). Pearce & Griffiths (1991) have shown that the meanders generally develop into cyclonic-anticyclonic eddy pairs: the anticyclonic wing (in particular) grows offshore to a width of order 200 km and may eventually "pinch-off" to form a free-standing eddy. Batteen & Rutherford (1990) have recently modelled the generation of meanders and eddies through both barotropic and baroclinic instability processes.

Between the meanders, the Current tends to flow along the shelf-break and upper slope as a jet-like current towards the south, and cyclonic eddies in the ambient water offshore can be associated with current speeds of over 80 cm s^{-1} (over 1.5 knots). The meanders do not appear to propagate along the coast. Similar structures occur along the south coast (Griffiths & Pearce 1985a); on at least one occasion, a warm eddy drifted southwards into the Southern Ocean (Griffiths & Pearce 1985b).

The western (offshore) boundary of the Leeuwin Current is generally well defined, with a temperature differential of 2 to 5°C between the warm Current water and that offshore, associated with a strong cyclonic shear zone (Cresswell & Golding 1980). The inshore boundary is less clearly defined as the thermal gradient is weaker. Nevertheless, small-scale (order 20 km) billows indicate zones of current shear and active exchange of water between the Current and the shelf water (Pearce & Griffiths 1991).

Interannual variability

Pearce & Phillips (1988) have demonstrated that annual mean coastal sealevels (which may be used as one indicator of the strength of the Leeuwin Current) fluctuate with ENSO (El Niño/Southern Oscillation) events. During ENSO years, relatively low coastal sealevels imply a weaker Leeuwin Current, and conversely, in anti-ENSO years, higher mean sealevels indicate stronger southwards flow. Pattiaratchi & Buchan (1991) have extended the analysis to show that coastal sealevels off Western Australia have been related to ENSO events since the turn of the century.

Temperature and salinity measurements along the outer shelf off Perth confirm that, during ENSO periods, the water along the outer shelf is relatively cooler and more saline than in anti-ENSO years, indicative of less tropical water being advected southwards by the Current (Pearce & Phillips 1988). Pearce & Phillips (1988) and Phillips *et al.* (1991) discuss the implications of this interannual fluctuation in flow for larval recruitment of the western rock lobster.

Conclusions

The Leeuwin Current has been shown to be quite different from the corresponding EBCs of the other two southern hemisphere oceans. Off Namibia and the Peru-Chile region there are cool northward currents, and the upwelling of nutrient-rich water results in highly productive waters on the continental shelf. Off Western Australia, by contrast, the Leeuwin Current transports warm tropical water southwards and (despite upwelling-favourable winds) there is no upwelling.

The difference seems to be largely associated with the flow of warm Pacific Ocean water through the Indonesian Archipelago, leading to a much stronger meridional pressure gradient off Western Australia than exists off Africa or South America.

Poleward under/countercurrents exist off southern Africa and the Peru-Chile region, but they are comparatively weak in comparison with the Leeuwin Current. Instead, there is an equatorwards undercurrent beneath the Leeuwin Current – this is not found along any other eastern boundary.

Interannual variability of coastal sealevels (which may be used as an indicator of the strength of the alongshore flow) is linked with ENSO events, such that the Leeuwin Current is relatively weak in ENSO years and stronger during anti-ENSO periods.

Acknowledgements I am indebted to Dr Vere Shannon and Dr Jane Huyer for helpful suggestions on the Benguela and Humboldt systems respectively, and to Dr George Cresswell, Dr Stuart Godfrey and Dr Chari Pattiaratchi for general comments. Richard Litchfield and Bert de Boer carried out the COADS programming. Ms Liz Jefferson drew the diagrams.

References

Andrews J C 1977 Eddy structure and the West Australian Current. Deep-Sea Res 24:1133-1148.

Bang N D & Andrews W R H 1974 Direct current measurements of an oceanic frontal jet in the upwell regime west of Cape Town. J Mar Res 32:405-417.

Batteen M L & Rutherford M J 1990 Modeling studies in the Leeuwin Current: the role of thermal forcing. J Phys Oceanogr 20:1484-1520.

Brattström H & Johanssen A 1983 Ecological and regional zoogeography of the marine benthic fauna of Chile. Reports of the Lund University Chile Expedition 1948-49, No 49. Sarsia 68:289-339.

Brockman C, Fahrbach E, Huyer A & Smith R L 1980 The poleward undercurrent along the Peru coast: 5 to 15°S. Deep-Sea Res 27:847-856.

Buys M E L 1957 Temperature variations in the upper 50 metres in the St Helena Bay area, September 1950 - August 1954. S Afr Div Fish Invest Rept 27: 113pp.

Cane M A 1983 Oceanographic events during El Niño. Science 222: 1189-1195.

Church J A, Cresswell G R & Godfrey J S 1989 The Leeuwin Current. In: Poleward flows along eastern ocean boundaries (eds S J Neshyba, C N K Mooers, R L Smith & R T Barber) Springer-Verlag, New York, 230-252.

Codispoti L A, Barber R T & Friederich G E 1989 Do nitrogen transformations in the poleward undercurrent off Peru and Chile have a globally significant influence? In: Poleward flows along eastern ocean boundaries (eds S J Neshyba, C N K Mooers, R L Smith & R T Barber) Springer-Verlag, New York, 281-314.

Cresswell G R 1991 The Leeuwin Current - observations and recent models. In: The Leeuwin Current: an influence on the coastal climate and marine life of Western Australia. (eds. AF Pearce and DI Walker). J Roy Soc WA 74:1-14.

Cresswell G R & Golding T J 1980 Observations of a south-flowing current in the southeastern Indian Ocean. Deep-Sea Res 27:449-466.

FAO 1981 Atlas of the living resources of the sea. FAO Fisheries Dept, 23pp + charts.

Gentilli J 1972 Ocean-atmosphere relations on the Western Australian coast. In: Proposal for marine environmental studies off the western coast of Australia (comp L C Brodie-Hall) CSIRO, 17-37.

Godfrey J S & Ridgway K R 1985 The large-scale environment of the poleward-flowing Leeuwin Current, Western Australia: longshore steric height gradients, wind stresses and geostrophic flow. J Phys Oceanogr 15:481-495.

Godfrey J S & Weaver A J 1991 Is the Leeuwin Current driven by Pacific heating and winds? Progr Oceanogr 27:225-272.

Griffiths R W & Pearce A F 1985a Instability and eddy pairs on the Leeuwin Current south of Australia. Deep-Sea Res 32:1511-1534.

Griffiths R W & Pearce A F 1985b Satellite images of an unstable warm eddy derived from the Leeuwin Current. Deep-Sea Res 32:1371-1380.

Gunther E R 1936 A report on oceanographical investigations in the Peru Coastal Current. Discovery Rep 13:107-276.

Hart T J & Currie R I 1960 The Benguela Current. Discovery Rept 31:123-298.

Huyer A, Knoll M, Paluszkiewicz T & Smith R L 1991 The Peru Undercurrent: a study in variability. Deep-Sea Res. 38 Suppl: S247-S271

Legeckis R & Cresswell G R 1981 Satellite observations of sea-surface temperature fronts off the coast of western and southern Australia. Deep-Sea Res 28:297-306.

Murphy R 1936 Oceanic birds of South America. 2 vols, Macmillan, New York.

Nelson G 1989 Poleward motion in the Benguela area. In: Poleward flows along eastern ocean boundaries (eds S J Neshyba, C N K Mooers, R L Smith & R T Barber) Springer-Verlag, New York, 110-130.

Nelson G & Hutchings L 1983 The Benguela upwelling area. Progr Oceanogr 12:333-356.

Neshyba S J, Mooers C N K, Smith R L & Barber R T (editors) 1989 Poleward flows along eastern ocean boundaries. Springer-Verlag, New York.

Pattiaratchi C B & Buchan S J 1991 Implications of long-term climate change for the Leeuwin Current. In: The Leeuwin Current: an influence on the coastal climate and marine life of Western Australia. (eds. A F Pearce and D I Walker) J Roy Soc WA 74:133-140.

Pearce A F & Griffiths R W 1991 The mesoscale structure of the Leeuwin Current. J Geophys Res. C96:16739-16757

Pearce A F & Phillips B F 1988 ENSO events, the Leeuwin Current, and larval recruitment of the western rock lobster. J Cons int Explor Mer 45:13-21.

Phillips B F, Pearce A F & Litchfield R 1991 The Leeuwin Current and larval recruitment to the rock (spiny) lobster fishery off Western Australia. In: The Leeuwin Current: an influence on the coastal climate and marine life of Western Australia. (eds. A F Pearce and D I Walker) J Roy Soc WA 74:93-100.

Quinn W H, Zopf D O, Short K S & Yang R T W K 1978 Historical trends and statistics of the Southern Oscillation, El Niño and Indonesian droughts. Fish Bull 76(3):663-678.

Reynolds R W 1982 A monthly averaged climatology of sea surface temperature. NOAA Tech Rep NWS 31:35 pp.

Shannon L V 1985 The Benguela ecosystem. Part 1. Evolution of the Benguela, physical features and processes. Oceanogr Mar Biol Ann Rev 23:105-182.

Shannon L V, Stander G H & Campbell J A 1973 Ocean circulation deduced from plastic drift cards. Rep S Afr Sea Fish Branch Invest Rep 108:31pp.

Shannon L V, Agenbag J J & Buys M E L 1987 Large- and mesoscale features of the Angola-Benguela front. S Afr J Mar Sci 5:11-34

Silva S N & Neshyba S 1979 On the southernmost extension of the Peru-Chile Undercurrent. Deep-Sea Res 26:1387-1393.

Smith R L 1983 Circulation patterns in upwelling regimes. In: Coastal upwelling (eds E Suess & J Thiede), Plenum Publ Corp:13-35.

Smith R L, Huyer A, Godfrey J S & Church J A 1991 The Leeuwin Current off Western Australia, 1986-87. J Phys Oceanogr 21: 323-345.

Tchernia P 1980 Descriptive regional oceanography. Pergamon Press 253 pp.

Thompson R O R Y 1984 Observations of the Leeuwin Current off Western Australia. J Phys Oceanogr 14:623-628.

Weaver A J & Middleton J H 1989 On the dynamics of the Leeuwin Current. J Phys Oceanogr 19:626-648.

Wooster W S & Reid J L 1963 Eastern boundary currents. In: The sea vol 2 (ed Hill M N) Pergamon Press: 253-279.

Wyrtki K 1963 The horizontal and vertical field of motion in the Peru Current. Bull Scripps Inst Oceanogr 8:313-345.

Wyrtki K 1966 Oceanography of the eastern equatorial Pacific. Oceanogr Mar Biol Ann Rev 4:33-68.

Wyrtki K 1971 Oceanographic atlas of the International Indian Ocean Expedition. National Science Foundation, Washington, 531pp.

Zuta S 1988 Variations in the mass field and currents off the Peru coast. Intergov Oceanogr Comm Tech Ser 33 "Time series of ocean measurements 4":55-75.